Arbitrary waveform synthesis by multiple harmonics generation and phasing in aperiodic optical superlattices

Wei-Hsun Lin[1,*] and A. H. Kung[1,2]

[1] *Institute of Atomic and Molecular Sciences, Academia Sinica, Taipei 10617, Taiwan, R.O.C.*
[2] *Department of Photonics, National Chiao Tung University, Hsinchu 30010, Taiwan, R.O.C.*
**wei.xun.lin@gmail.com*

Abstract: The process of generating periodic optical waveforms includes the generation and phasing of several harmonics of a fundamental frequency. In this work, we show that simultaneous generation and phasing of the harmonics can be performed in a monolithic aperiodic optical superlattice (AOS). Stable periodic waveforms can thus be delivered to a predetermined location by simply sending a laser beam through a properly designed and fabricated AOS crystal. A detailed mathematical description for generating the domain pattern in such an AOS crystal is given and the process is numerically demonstrated. The waveform that is generated from a monolithic AOS is highly reproducible and phase stable. We also use propagation in air as an example to show how any predictable phase and amplitude modifications such as air dispersion that will alter the desired waveform can be pre-compensated in the design phase of the AOS crystal.

OCIS codes: (320.5540) Pulse shaping; (230.5298) Photonic crystals; (190.4160) Multiharmonic generation.

References and links

1. Z. Jiang, D. S. Seo, S.-D. Yang, D. E. Leaird, R. V. Roussev, C. Langrock, M. M. Fejer, and A. M. Weiner, "Four-User, 2.5-Gb/s, Spectrally Coded OCDMA System Demonstration Using Low-Power Nonlinear Processing," J. Lightwave Technol. **23**(1), 143–158 (2005).
2. M. C. Stowe, F. C. Cruz, A. Marian, and J. Ye, "High resolution atomic coherent control via spectral phase manipulation of an optical frequency comb," Phys. Rev. Lett. **96**(15), 153001 (2006).
3. A. Baltuska, Th. Udem, M. Uiberacker, M. Hentschel, E. Goulielmakis, Ch. Gohle, R. Holzwarth, V. S. Yakovlev, A. Scrinzi, T. W. Hänsch, and F. Krausz, "Attosecond control of electronic processes by intense light fields," Nature **421**(6923), 611–615 (2003).
4. A. M. Weiner, J. P. Heritage, and E. M. Kirschner, "High-resolution femtosecond pulse shaping," J. Opt. Soc. Am. B **5**(8), 1563–1572 (1988).
5. J. K. Ranka, R. S. Windeler, and A. J. Stentz, "Visible continuum generation in air-silica microstructure optical fibers with anomalous dispersion at 800 nm," Opt. Lett. **25**(1), 25–27 (2000).
6. P. B. Corkum, "Plasma perspective on strong field multiphoton ionization," Phys. Rev. Lett. **71**(13), 1994–1997 (1993).
7. S. E. Harris, and A. V. Sokolov, "Subfemtosecond Pulse Generation by Molecular Modulation," Phys. Rev. Lett. **81**(14), 2894–2897 (1998).
8. T. W. Hänsch, "A proposed sub-femtosecond pulse synthesizer using separate phase-locked laser oscillators," Opt. Commun. **80**(1), 71–75 (1990).
9. I. V. Shutov, and A. S. Chirkin, "Consecutive high-order harmonic generation and formation of subfemtosecond light pulses in aperiodical nonlinear photonic crystals," Phys. Rev. A **78**(1), 013827 (2008).
10. M. Y. Shverdin, D. R. Walker, D. D. Yavuz, G. Y. Yin, and S. E. Harris, "Generation of a single-cycle optical pulse," Phys. Rev. Lett. **94**(3), 033904 (2005).
11. W. J. Chen, Z. M. Hsieh, S. W. Huang, H. Y. Su, C. J. Lai, T. T. Tang, C. H. Lin, C. K. Lee, R. P. Pan, C. L. Pan, and A. H. Kung, "Sub-single-cycle optical pulse train with constant carrier envelope phase," Phys. Rev. Lett. **100**(16), 163906 (2008).
12. Z. Jiang, C.-B. Huang, D. E. Leaird, and A. M. Weiner, "Optical arbitrary waveform processing of more than 100 spectral comb lines," Nat. Photonics **1**(8), 463–467 (2007).
13. N. Bloembergen, *Nonlinear Optics* (World Scientific, 1996).
14. S. N. Zhu, Y. Y. Zhu, and N. B. Ming, "Quasi–Phase-Matched Third-Harmonic Generation in a Quasi-Periodic Optical Superlattice," Science **278**(5339), 843–846 (1997).

#112976 - $15.00 USD Received 19 Jun 2009; revised 28 Jul 2009; accepted 28 Jul 2009; published 28 Aug 2009

15. D. H. Jundt, M. M. Fejer, and R. L. Byer, "Optical Properties of Lithium-Rich Lithium Niobate Fabricated by Vapor Transport Equilibration," IEEE J. Quantum Electron. **26**(1), 135–138 (1990).
16. E. Peck, and K. Reeder, "Dispersion of Air," J. Opt. Soc. Am. **62**(8), 958–962 (1972).

1. Introduction

In recent years there is a lot of interest in the synthesis of arbitrary optical waveforms because of their potential application in telecommunication [1], quantum control [2], and ultrafast electronic processing [3]. It is now understood that there are two essential requirements toward achieving full control in the synthesis of periodic arbitrary optical waveforms. The first one is the generation of a broad spectrum consisting of a series of commensurate harmonic components. The generated frequency components serve as the building blocks of any desired waveform. The other requirement is to have the ability to manipulate the phase and amplitude of each harmonic to achieve the desired waveform. To obtain such a periodic waveform, the phase of each harmonic must be adjusted to satisfy the condition

$$\varphi_n = \varphi_{CE} + n\varphi_m, \tag{1}$$

where φ_{CE} is the carrier-envelope phase and φ_m is a uniform phase difference between adjacent components. When both requirements are satisfied, an arbitrary periodic waveform can be produced by superposition of the components of the series [4].

Generally these requirements are satisfied in consecutive steps. A phase coherent Fourier spectrum is first generated using methods such as self-phase modulation in nonlinear photonic crystal fiber [5], high harmonic generation from ultrafast lasers [6], molecular modulation [7], or multiple harmonics generation [8,9]. In some of these methods periodic ultrashort pulse trains are formed at the location where the phase-coherent spectrum is produced. Yet material dispersion and propagation phase shifts distort the waveform after exiting the generator. Hence generally the generation is followed by some form of a phase compensation scheme that employs grating pairs, prisms, and/or spatial light modulators to adjust the phase and amplitude of the series components to arrive at the desired result [10–12].

The optical Fourier synthesizer using multiple harmonics was first proposed by Hänsch [8], who phase-locked two lasers to construct a frequency comb, employing frequency mixing processes in nonlinear crystals. The frequency mixing process and the phase-locked lasers guarantee a stable phase difference between every pair of adjacent frequency components. Waveforms can then be synthesized subsequently by monitoring and shifting the phase of each frequency component. In this paper we describe an approach utilizing an aperiodic optical superlattice (AOS) to simultaneously generate and phase the spectrum such that periodic electromagnetic waveforms of any predetermined shape can be delivered to a specified location in a single setting.

It is well-known that quasi-phase-matched nonlinear interaction can be achieved by periodically modulating the second order nonlinearity $d^{(2)}$ to create a nonlinear reciprocal lattice vector in a crystal that offsets the phase-mismatch of a nonlinear interaction in the medium [13]. By introducing aperiodic or quasi-periodic modulation Zhu and associates first showed that two lattice vectors can be created in one crystal to provide simultaneous quasi-phase-matched second and third harmonic generation in a superlattice [14]. Recently, Shutov and Chirkin advanced the technique to show by simulation that several harmonics can be generated in an AOS to provide a broad comb of coherent frequencies [9]. They proposed AOS designs that optimize the efficiency of each harmonic generation stage to produce up to 8 consecutive harmonics, the superposition of which gives pulses of ultimate duration at some fixed interaction length determined and limited by the dispersion properties of the AOS. However, additional steps are required to compensate any distortion to the pulse when delivering it to the location where it will be applied. Here we expand on the idea of using an AOS to propose and numerically demonstrate a device that allows the delivery of an ultrafast periodic waveform to a predetermined location. For example, a specific waveform can be delivered directly to a heterojunction of a nanoscale photoelectronic device where the ultrafast

#112976 - $15.00 USD Received 19 Jun 2009; revised 28 Jul 2009; accepted 28 Jul 2009; published 28 Aug 2009

dynamics of the electron and hole carriers are to be characterized. This is accomplished by engineering the phase and amplitude of $d^{(2)}$ of an AOS so that the AOS will provide the required comb of harmonics that Fourier synthesizes to the desired waveform at that location.

2. Basic principle of the model

We begin with the equation for second order nonlinear frequency conversion

$$\frac{\partial E_r}{\partial z} = -i \sum_{\omega_p + \omega_q = \omega_r} \frac{\omega_r d^{(2)}(z)}{c n_r} E_p E_q \exp(-i\Delta k_{(rpq)} z), \tag{2}$$

where $E_{n=r,p,q}$ is the complex amplitude $E_n(z)e^{i\varphi_n}$ of the time-dependent electric field $E_n(z,t) = E_n(z)e^{i(\omega_n t - k_n z + \varphi_n)}$, z is the direction of propagation, $d^{(2)}(z)$ is the second order nonlinear coefficient, ω_n and $k_n = \omega_n n_n / c$ are the frequency and wavevector of E_n, n_n is refractive index, and $\Delta k_{(rpq)} = k_p + k_q - k_r$ is the photon momentum mismatch.

Successful periodic waveform synthesis requires the formation of a commensurate series of harmonics that begins with the fundamental frequency ω_1 and the n th component is $\omega_n = n\omega_1$. These harmonics can be generated in a series of processes described by Eq. (2). To calculate the phase of each harmonic at z, we express Eq. (2) as

$$\frac{\partial E_r}{\partial z} = -i \sum_{(rpq)} \frac{\omega_r}{c n_r} \tilde{d}_{(rpq)} E_p E_q, \tag{3}$$

where the RHS is the sum of all possible channels $\omega_p + \omega_q \to \omega_r$ which contribute to the generation of E_r, and $\tilde{d}_{(rpq)}$ is defined as a channel specific effective second order nonlinear coefficient of the medium over a distance L,

$$\tilde{d}_{(rpq)} \equiv \tilde{d}(\Delta k_{(rpq)}) = \frac{1}{L}\int d^{(2)}(z)\exp(-i\Delta k_{(rpq)} z)dz. \tag{4}$$

In conventional quasi-phase-matched harmonic generation $d^{(2)}(z)$ is designed to optimize the generation efficiency so that $\tilde{d}_{(rpq)}$ is real. By constructing $\tilde{d}_{(rpq)}$ to have a nonzero phase, the output E_r will carry an additional phase $\varphi_{\tilde{d}_{(rpq)}}$. Hence through the design of $d^{(2)}(z)$ we can impose a phase that is required on each harmonic output to produce the designed waveform waveform.

The connection between $\varphi_{\tilde{d}_{(rpq)}}$ and the phase of each harmonic is shown as follows. While there can be many possible combinations of p and q in Eq. (4) we shall simplify the situation by choosing $p = 1$ and $q = r - 1$, that is $\omega_1 + \omega_{r-1} \to \omega_r$, to be the dominating channels. With this choice, every harmonic is produced by sum mixing that includes E_1. The phase of the n th harmonic generated is given by:

$$\begin{aligned} \varphi_n^{(final)} &= \varphi_n + \phi_n = -\frac{\pi}{2} + \varphi_{\tilde{d}_{(n(n-1)1)}} + \varphi_{n-1} + \varphi_1 + \phi_n, \\ \varphi_1^{(final)} &= \varphi_1 + \phi_1, \end{aligned} \tag{5}$$

where φ_n is the phase of E_n at the exit end of the crystal, $\varphi_n^{(final)}$ is the required phase of E_n at the desired location and ϕ_n represents the additional phase shift modulo to 2π acquired by E_n during propagation from the crystal exit to the final destination. In a periodic waveform,

#112976 - $15.00 USD Received 19 Jun 2009; revised 28 Jul 2009; accepted 28 Jul 2009; published 28 Aug 2009

the CEP is given by $\varphi_{CE} = 2\varphi_1 - \varphi_2 = \varphi_1 + \varphi_2 - \varphi_3 = \ldots$, therefore if we design $d^{(2)}(z)$ of a crystal such that

$$\frac{\pi}{2} - \varphi_{\tilde{d}_{(211)}} + 2\phi_1 - \phi_2 = \frac{\pi}{2} - \varphi_{\tilde{d}_{(321)}} + \phi_1 + \phi_2 - \phi_3 = \ldots, \tag{6}$$

then all the harmonics will be phase-coherent to give a CEP that equals $\frac{\pi}{2} - \varphi_{\tilde{d}_{(211)}} + 2\phi_1 - \phi_2$. Note that the CEP is not affected by the absolute phase of the fundamental frequency φ_1. As can be seen from Eq. (5), phase fluctuation of the input laser, $\varphi_1 \to \varphi_1 + \Delta\varphi_1$, will only result in a phase shift, $n\Delta\varphi_1$, for the nth component, $\varphi_n^{(final)} \to \varphi_n^{(final)} + n\Delta\varphi_1$ and then a time shift $\Delta\varphi_1 / \omega_1$ to the overall synthesized waveform. Since $\Delta\phi_1$ is less than 2π and ω_1 is in the optical range, the shift is insignificant so long as the input consists of more than a few cycles.

3. Design algorithm

The design of an AOS that can deliver a desired waveform will amount to finding a solution for $d^{(2)}(z)$ by solving numerically Eq. (2) with an initial input of $E_1 = E(0)$ and $E_n = 0$, $i \neq 1$ and a given set of final E field amplitudes and phases as the boundary conditions. Shutov describes a generalized sign function

$$d^{(2)}(\mathsf{z}) \propto \mathrm{sgn}\Big(\sum_{(rpq)}^{N} a_{(rpq)} \sin(\Delta k_{(rpq)}\mathsf{z} + \zeta_{(rpq)})\Big), \tag{7}$$

where $a_{(rpq)}$ and $\zeta_{(rpq)}$ are amplitude and phase parameters of the harmonic modulation. $\Delta k_{(rpq)}$ in the sine function is to include the quasi-phase-matching of the channel $\omega_p + \omega_q \to \omega_r$ in the lattice periodicity to characterize the periodical dependence of $d^{(2)}(z)$ for N simultaneous QPM processes. We take into consideration that there is a minimum domain length that can reliably be fabricated in the AOS and modify Eq. (7) to include this minimum length. We further add a criterion that the width of each domain is equal to an integral multiple of this minimum width in the superlattice to arrive at the following design function for the crystal:

$$d^{(2)}(z) \propto \mathrm{sgn}\Big(\int_{\lfloor z/l-1 \rfloor l}^{\lfloor z/l \rfloor l} \sum_{(rpq)}^{N} a_{(rpq)} \cos(\Delta k_{(rpq)} z' + \zeta_{(rpq)}) dz'\Big), \tag{8}$$

where l is the length of a block that equals to the minimum domain width, $\lfloor \mathsf{z}/l \rfloor$ is a floor function which returns the greatest integer less than or equal to z/l, and $a_{(rpq)}$ and $\zeta_{(rpq)}$ are generation parameters which determine the amplitude and phase of the spectrum of the final poling sequence. The sum of all different frequency terms is integrated over the block length from $\lfloor \mathsf{z}/l - 1 \rfloor l$ to $\lfloor \mathsf{z}/l \rfloor l$. The corresponding sign function returns the polarization direction of the block.

By iteratively adjusting the values of $a_{(rpq)}$ and $\zeta_{(rpq)}$, it is possible to produce a solution for $d^{(2)}(\mathsf{z})$ that will result in predetermined output electric field amplitudes and phases. In this algorithm the calculated amplitude $\left|\tilde{d}_{(rpq)}\right|$ is mainly affected by $a_{(rpq)}$ and the phase $\varphi_{\tilde{d}_{(rpq)}}$ by $\zeta_{(rpq)}$. This can be seen by recognizing in Eq. (8) that inclusion of $\zeta_{(rpq)}$ is equivalent to introducing an offset to the initial phase $\Delta k_{(rpq)}$ of the frequency components in

#112976 - $15.00 USD Received 19 Jun 2009; revised 28 Jul 2009; accepted 28 Jul 2009; published 28 Aug 2009

the domain pattern. This feature makes the algorithm very robust when searching for the final solution since the amplitude and phase of the output electric field can be considered separately. Note that the choice of the form of Eq. (8) is somewhat arbitrary. Any solution that has a basic sinusoidal form will work, as different forms of sinusoids will only result in a shift or a sign change between $\zeta_{(rpq)}$ and the calculated value of $\varphi_{\tilde{d}_{(rpq)}}$. For convenience we have chosen the cosine function so that the calculated $\varphi_{\tilde{d}_{(rpq)}}$ will have the same sign as the generation parameters of the phase $\zeta_{(rpq)}$.

A numerical procedure based on simulated annealing algorism is used to generate the poling pattern of the crystal by first selecting a length for the domain block. The value of each $\varphi_{\tilde{d}_{(rpq)}}$ can be estimated from the desired value of the final CEP using Eq. (6). The initial generation parameters $a_{(rpq)}$ are then arbitrarily chosen to calculate a $d^{(2)}(z)$ with Eq. (8). The $d^{(2)}(z)$ that results from this calculation is fed into Eq. (2) to obtain E_n for comparison with the values of the fields of the desired waveform. If the root mean square of the difference of the calculated fields and the desired fields is larger than a prescribed value the procedure is repeated using a randomly chosen set of $a_{(rpq)}$ until the calculated and the desired E fields agree to within an acceptable value.

4. Numerical examples

We demonstrate the utility of the above procedure with a few numerical examples. We use lithium niobate at 100 °C as the nonlinear medium. In the first example we aim to produce a sawtooth waveform at the crystal exit by the superposition of the first five harmonics with channels: $\omega_1+\omega_1\rightarrow\omega_2$, $\omega_1+\omega_2\rightarrow\omega_3$, $\omega_1+\omega_3\rightarrow\omega_4$, $\omega_1+\omega_4\rightarrow\omega_5$. In correspondence to our previous work [11], we choose 2.406 μm as the fundamental wavelength. The phase mismatch of each channel, $\Delta k_{(rpq)}$, is listed in Table 1.

Table 1. Phase mismatch of selected processes[a]

Channel	Δk ($1/\mu$m)	$2\pi/\Delta k$ (μm)
$\omega_1+\omega_1\rightarrow\omega_2$	0.22380283	28.074647
$\omega_1+\omega_2\rightarrow\omega_3$	0.31866532	19.717192
$\omega_1+\omega_3\rightarrow\omega_4$	0.53402295	11.765759
$\omega_1+\omega_4\rightarrow\omega_5$	0.89204589	7.0435673
$\omega_2+\omega_3\rightarrow\omega_5$	1.2022660	5.2261190
$\omega_2+\omega_5\rightarrow\omega_7$	3.7292894	1.6848211

[a]In lithium niobate at 100 °C and $\lambda_1^{(vacuum)}=2.406$ μm, calculated using refractive index data from Ref [15].

We choose to set the length of each block at $7.04/3=2.35$ μm where 7.04 μm is the smallest QPM period of all channels used in this process (as shown in the first four rows in Table 1), i.e., $2\pi/(k_5-k_4-k_1)$. The total number of blocks is 2475. Hence the crystal length is approximately 6 mm. We use the plane wave approximation and assume a rectangular temporal input pulse with an intensity of 100 MW/cm^2 and assume the initial phase $\varphi_1=0$. After several iterations we obtain a set of generation parameters $a_{(211)}=1.000$, $a_{(321)}=0.996$, $a_{(431)}=1.174$, $a_{(541)}=1.294$ and $\zeta_{(211)}=\zeta_{(321)}=\zeta_{(431)}=\zeta_{(541)}=0$ that results in a calculated

#112976 - $15.00 USD Received 19 Jun 2009; revised 28 Jul 2009; accepted 28 Jul 2009; published 28 Aug 2009

field amplitude ratio of 1.000:0.501:0.340:0.252:0.194 for the 1st to 5th harmonics, which is close to the desired 1:1/2:1/3:1/4:1/5 for a square waveform. The absolute values of the corresponding effective second order nonlinear coefficients $\left|\tilde{d}(\Delta k)\right|$ is calculated to be 42%, 41%, 45% and 39% of a perfectly quasi-phase-matched periodic poled nonlinear crystal. The evolution of the E fields and the calculated spectrum of $\left|\tilde{d}(\Delta k)\right|$ of the aperiodic pattern generated with this set of parameters are shown in Fig. 1.

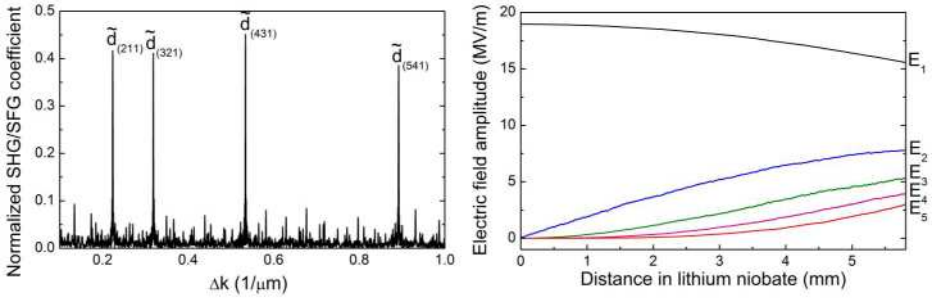

Fig. 1. (left frame) Absolute values of the normalized effective second order nonlinear coefficients $\left|\tilde{d}(\Delta k)\right|$ calculated from Eq. (4) of the designed aperiodic optical superlattice and (right frame) simulation results of the electric field evolution in the designed AOS.

From Eqs. (2) and (8) we expect that by setting all $\zeta_{(rpq)} = 0$, then all $\varphi_{\tilde{d}_{(rpq)}}$ will be 0. The calculated values of $\varphi_{\tilde{d}_{(211)}}$, $\varphi_{\tilde{d}_{(321)}}$, $\varphi_{\tilde{d}_{(431)}}$, and $\varphi_{\tilde{d}_{(541)}}$ are $0.0002\,\pi$, $0.0003\,\pi$, $0.0061\,\pi$, $-0.0022\,\pi$, respectively, which match well with the expected values of 0 to within $0.006\,\pi$. From Eq. (6) we get $\varphi_{CE} = 0.5\pi - \varphi_{\tilde{d}} = 0.5\pi$ and $\varphi_m = \varphi_1 - \varphi_{CE} = -0.5\pi$. The predicted phases of the harmonics are $\varphi_2 = -0.5\pi$, $\varphi_3 = -1.0\pi$, $\varphi_4 = -1.5\pi$ and $\varphi_5 = -2.0\pi$. The actual simulation gives $\varphi_1 = -0.0007\pi$, $\varphi_2 = -0.5019\pi$, $\varphi_3 = -1.0030\pi$, $\varphi_4 = -1.4983\pi$ and $\varphi_5 = -2.0123\pi$, which also match well with the prediction.

This algorithm works for any value of the CEP. We used several sets of values of $\zeta_{(rpq)}$: $\zeta_{(rpq)}$ equaling to 0, or $\pi/2$, or π, or $3\pi/2$ respectively and repeated the calculation. Note that each set of $\zeta_{(rpq)}$ corresponds to a different AOS design. The phase evolution inside the lithium niobate crystal for each set of $\zeta_{(pqr)}$ and the corresponding envelope and electric field intensity of the waveforms are shown in Fig. 2. We see that the phases converge rather quickly to a value that agrees with the desired values in all cases.

#112976 - $15.00 USD Received 19 Jun 2009; revised 28 Jul 2009; accepted 28 Jul 2009; published 28 Aug 2009

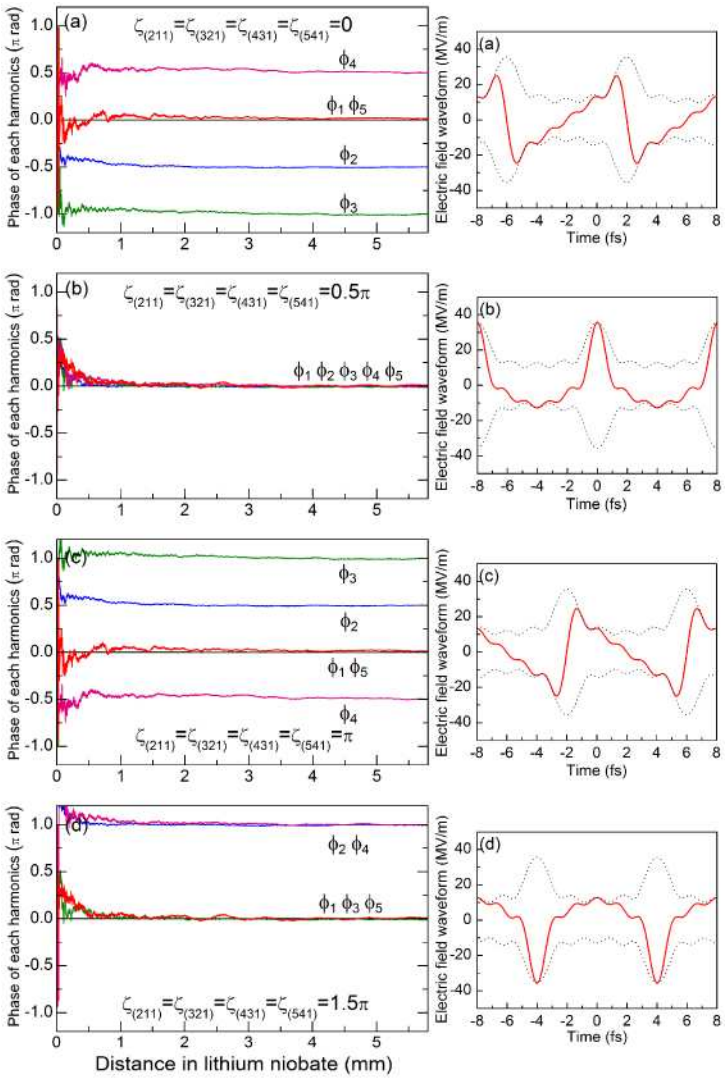

Fig. 2. (large frames) Simulation results of the phase evolution inside the designed AOS and (small frames) the corresponding waveforms (solid curve) and envelopes (dotted curve). (a) For AOS generation parameters of phase $\zeta_{(211)} = \zeta_{(321)} = \zeta_{(431)} = \zeta_{(541)} = 0$, simulation results agree with expected values $\varphi_{CE} = 0.5\pi$ and $\varphi_m = -0.5\pi$ .For $\zeta_{(211)} = \zeta_{(321)} = \zeta_{(431)} = \zeta_{(541)} = 0.5\pi$, $1.0\,\pi$ and $1.5\ \pi$ from (b) to (d), the expected values are (b) $\varphi_{CE} = 0$, $\varphi_m = 0$, (c) $\varphi_{CE} = -0.5\pi$, $\varphi_m = 0.5\pi$, (d) $\varphi_{CE} = -1.0\pi$, $\varphi_m = 1.0\pi$, respectively. In a stable periodic waveform, φ_{CE} affects the shape of the waveform, and φ_m produces a timeshift. This is confirmed with the results shown in the small frame figures on the right where the envelopes shift sequentially by 1/4 period from (a) to (d), which is due to the $0.5\,\pi$ phase shift of φ_m from one figure to the next.

In the event the externally imposed phase shift ϕ_n of the n th harmonics is not zero, we can compensate that by changing the values of $\zeta_{(rpq)}$ in Eq. (8). This will be the case, for instance, if we want to have a sawtooth waveform 1 m away instead of right at the crystal exit. Assuming plane wave propagation in air, then using published data on the refractive index of

#112976 - $15.00 USD Received 19 Jun 2009; revised 28 Jul 2009; accepted 28 Jul 2009; published 28 Aug 2009

air [16], the phase evolution of the above harmonics are calculated to be $-831484.366\,\pi$, $-1662970.062\,\pi$, $-24944584.580\,\pi$, $-33259510.110\,\pi$, $-41574493.192\,\pi$, which correspond to $\phi_n = -0.366\pi$, $-0.062\,\pi$, $-0.580\,\pi$, $-0.110\,\pi$, $-1.192\,\pi$, for $n = 1$, 2, 3, 4, 5, respectively. From Eq. (6) we can compensate this dispersion by shifting $\zeta_{(211)}$ by $-0.366\pi \times 2 - (-0.062\pi)$, $\zeta_{(321)}$ by $-0.366\pi - 0.062\pi - (-0.580\pi)$ and so on. Solving Eq. (8) with this set of $\zeta_{(rpq)}$ then results in a new AOS design that gives a sawtooth waveform located at 1 m away from the crystal, as shown in Fig. 3. The waveform at the crystal end immediately after the generation process has a very different form compared to Fig. 2.

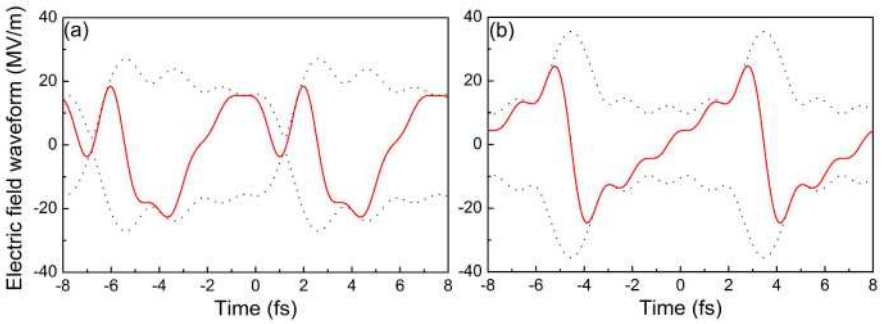

Fig. 3. Generated electromagnetic waveform (solid curve) and the corresponding envelope (dotted curve) which are (a) at the crystal exit and (b) at 1 m away from the crystal exit. The generation amplitude parameters are set to $a_{(211)} = 1.000$, $a_{(321)} = 0.996$, $a_{(431)} = 1.174$, $a_{(541)} = 1.294$, which are the same as those for calculating Fig. 2. The generation phase parameters are set to $\zeta_{(211)} = 1.332\pi$, $\zeta_{(321)} = 0.030\pi$, $\zeta_{(431)} = 0.186\pi$, $\zeta_{(541)} = 1.942\pi$ to compensate the phase distortion due to dispersion in air.

The algorithm we have described indeed is very versatile. For many common waveforms such as the square wave or the triangular waveform, only a subset of the harmonics is needed to synthesize the desired waveform. A suitable generation path can be chosen with just the necessary harmonics to optimize the field power usage and remove the need to filter out unnecessary harmonics. To demonstrate the point, we designed an AOS pattern for generating a square wave. The Fourier components of a square wave have only odd frequency terms. For our example we employ a total of five harmonics ω_n, $n = 1$, 2, 3, 5, 7 with the channels $\omega_1 + \omega_1 \to \omega_2$, $\omega_1 + \omega_2 \to \omega_3$, $\omega_2 + \omega_3 \to \omega_5$, $\omega_2 + \omega_5 \to \omega_7$. ω_2 is required in order to generate the higher harmonics and is expected to exhaust its energy before propagating into free space. The phase mismatch $\Delta k_{(rpq)}$ of each channel is listed in Table 1. The simulation uses a lithium niobate crystal that has 104000 blocks. The block length is 0.6 μ m. The input fundamental intensity is 100 MW/cm^2. After several iterations we obtain the generation amplitude parameters to be $a_{(211)} = 1.000$, $a_{(321)} = 2.188$, $a_{(532)} = 12.119$, $a_{(752)} = 21.416$. Simulation shows that the normalized amplitudes of the 1st, 2nd, 3rd, 5th and 7th harmonics at the output are 1.000, 0.002, 0.343, 0.204, 0.140, respectively. The generated 2nd harmonic amplitude is less than 0.2% of the fundamental, showing that it has been effectively converted to the higher odd harmonics for the square wave. The waveforms corresponding to a few different CEPs are plotted in Fig. 4. Note that only $\varphi_{CE} = 0.5\pi$ gives a square waveform.

#112976 - $15.00 USD Received 19 Jun 2009; revised 28 Jul 2009; accepted 28 Jul 2009; published 28 Aug 2009

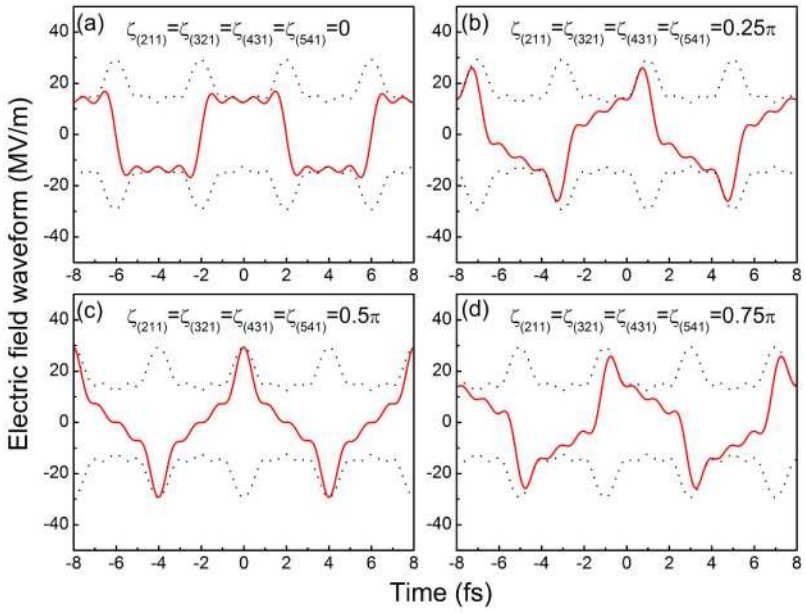

Fig. 4. Plots of simulated waveforms (solid curve) and envelopes (dotted curve). The generation amplitude parameters are set to $a_{(211)}=1.000$, $a_{(321)}=2.188$, $a_{(532)}=12.119$, $a_{(752)}=21.416$ and the generation phase parameters are set to $\zeta_{(211)}=\zeta_{(321)}=\zeta_{(431)}=\zeta_{(541)}=0$, 0.25 π , 0.5 π , 0.75 π from (a) to (d) respectively. From Eq. (8) and with $\varphi_1=0$, it can be predicted that φ_{CE} will change from 0.5 π to –0.25 π . The expected values of the CEP are (a) $\varphi_{CE}=0.5\pi$, $\varphi_m=-0.5\pi$. (b) $\varphi_{CE}=0.25\pi$, $\varphi_m=-0.25\pi$. (c) $\varphi_{CE}=0$, $\varphi_m=0$. (d) $\varphi_{CE}=-0.25\pi$, $\varphi_m=0.25\pi$, which agree with above waveforms.

5. Discussion

Many physical processes are sensitive to the form of the electric field. Meanwhile the CEP affects the time evolution of the electric field waveforms. These waveforms will be time-invariant if the CEP is constant. In general, electric fields experience phase shifts and amplitude modulations that distort the waveform. If the shifts and modulations are predictable, such as if they originate from propagation through a dispersive medium, Gouy phase shift, reflection from optics surfaces, etc. then they can be pre-compensated in the design phase of the AOS domain pattern by including the shifts and modulations in the iterative process. In this way we can deliver the desired waveform to any predetermined location.

An advantage of employing the AOS is that all the necessary steps in waveform synthesis, including broadband frequency generation, and amplitude and phase modulation are all completed in a monolithic crystal so that the resulting waveform will be very stable and reproducible. One can conceive many important applications for such highly stable and reproducible waveforms. For example, measurements that are highly repetitious, correlation measurements that require an ultrafast standard or probe, and heterodyne measurements that use an ultrafast oscillator would all benefit from having stable waveforms generated from such an AOS. On the other hand, the AOS approach has the severe restriction that only one particular waveform can be obtained from each AOS design and for one input intensity. As such, stable, CW or quasi-CW high power lasers are preferred to provide the fundamental frequency input. Precise knowledge of the refractive index of the crystal and a tight

#112976 - $15.00 USD Received 19 Jun 2009; revised 28 Jul 2009; accepted 28 Jul 2009; published 28 Aug 2009

temperature control must be available for an accurate waveform. The maximum number of harmonics which can be generated simultaneously is limited by the transmission bandwidth of the crystal and the fact that the poling of crystal domain widths of less than 1 μm over any useful length is unrealistic with today's poling technology. This last restriction can be somewhat mitigated by introducing high order QPM or using a longer fundamental wavelength.

In summary we have described the synthesis of periodic waveforms using a monolithic AOS. An algorithm to design the AOS is proposed and verified by numerical simulation. The AOS will enable us to create a desired electric waveform and deliver it to a predetermined location. The approach offers a simple and compact solution to consistently and reliably producing such waveforms for many interesting applications.

Acknowledgments

We thank Chao-Kuei Lee for helpful discussions. This work was supported by the Academia Sinica and the National Science Council of the R.O.C. under the Nanoscience and Technology Program.

#112976 - $15.00 USD Received 19 Jun 2009; revised 28 Jul 2009; accepted 28 Jul 2009; published 28 Aug 2009